Journal Pre-proof

Prenatal testosterone exposure induces insulin resistance, uterine oxidative stress and pro-inflammatory status in rats

Silvana Rocío Ferreira, Alicia Alejandra Goyeneche, María Florencia Heber, Giselle Adriana Abruzzese, Maria José Ferrer, Carlos Marcelo Telleria, Alicia Beatriz Motta

PII: S0303-7207(20)30347-6

DOI: https://doi.org/10.1016/j.mce.2020.111045

Reference: MCE 111045

To appear in: *Molecular and Cellular Endocrinology*

Received Date: 31 May 2020

Revised Date: 7 August 2020

Accepted Date: 30 September 2020

Please cite this article as: Ferreira, Silvana.Rocí., Goyeneche, A.A., Heber, Marí.Florencia., Abruzzese, G.A., Ferrer, Maria.José., Telleria, C.M., Motta, A.B., Prenatal testosterone exposure induces insulin resistance, uterine oxidative stress and pro-inflammatory status in rats, *Molecular and Cellular Endocrinology* (2020), doi: https://doi.org/10.1016/j.mce.2020.111045.

Prenatal testosterone exposure induces insulin resistance, uterine oxidative stress and pro-inflammatory status in rats.

Silvana Rocío Ferreira, PhD[1a*]; Alicia Alejandra Goyeneche, PhD[2]; María Florencia Heber, PhD[1b]; Giselle Adriana Abruzzese, PhD[1]; Maria José Ferrer[1]; Carlos Marcelo Telleria PhD[2,#]; Alicia Beatriz Motta, PhD[1,#].

[1]Laboratorio de Fisio-Patología Ovárica, Centro de Estudios Farmacológicos y Botánicos (CEFYBO), Consejo Nacional de Investigaciones Científicas y Técnicas (CONICET), Facultad de Medicina, Universidad de Buenos Aires (UBA), Argentina.

[2]Experimental Pathology Unit, Department of Pathology, Faculty of Medicine, McGill University, 3775 University Street, Montreal, QC H3A 2B4, Canada.

[a]Present address: Institut de Recherches Cliniques de Montréal, 110 av. des Pins Ouest, Montréal, QC, Canada H2W1R7. [b]Present address: Developmental Biology Laboratory, Malopolska Centre of Biotechnology at Jagiellonian University, str Gronostajowa 7a, 30-348, Krakow, Poland. 2

***Corresponding Author:** Silvana R. Ferreira - Laboratorio de Fisio-Patología Ovárica, Centro de Estudios Farmacológicos y Botánicos (CEFYBO), Consejo Nacional de Investigaciones Científicas y Técnicas (CONICET), Facultad de Medicina, Universidad de Buenos Aires (UBA) Paraguay 2155, Buenos Aires, Argentina, C1121ABG. Telephone: +54 11 5285-3602.
E-mail: silvanarocioferreira@gmail.com

[#]Co-principal investigators; these authors jointly supervised this work.

Abstract

Prenatal androgen excess is considered one of the main causes of the development of polycystic ovary syndrome. In this study, we investigated the effect of prenatal hyperandrogenization (PH) on the physiology of the adult uterine tissue using a murine model of fetal programming caused by androgen excess in adult female rats. Pregnant rats were hyperandrogenized with testosterone and female offspring were studied when adult. Our results showed that PH leads to hyperglycemia and hyperinsulinemia. Consequently, PH developed insulin resistance and a systemic inflammatory state reflected by increased C-reactive protein. In the uterine tissue, levels of PPAR gamma—an important metabolic sensor in the endometrium—were found to be impaired. Moreover, PH induced a pro-inflammatory and an unbalanced oxidative state in the uterus reflected by increased COX-2, lipid peroxidation, and NF-kB. In summary, our results revealed that PH leads to a compromised metabolic state likely consequence of fetal reprogramming.

Keywords: Prenatal hyperandrogenization, uterus, inflammation, oxidative stress, fetal programming.

1. Introduction

Polycystic ovary syndrome (PCOS) is a multifactorial endocrinopathy among women at reproductive age and the major cause of anovulatory infertility (Joham et al., 2015); its incidence is as high as 5-15% (Li et al., 2018). PCOS diagnosis comprises combinations of female hyperandrogenism, oligo- or anovulation, and polycystic ovaries. The etiology of PCOS remains unknown; however, current hypotheses propose that prenatal androgen excess during intrauterine life could lead to the development of the syndrome. It is important to point out that while PCOS patients present a high rate of spontaneous miscarriage and are often infertile mainly due to ovulation failure, if ovulation is restored, pregnancy rates still remain low (Badawy and Elnashar, 2011; Elnashar, 2011; Messinis, 2005). Adverse reproductive outcomes

could be attributed to a failure in the endometrial receptivity (Lopes et al., 2011) necessary for successful embryo implantation (Amjadi et al., 2018; Matsuzaki et al., 2017).

It is apparent that a link between PCOS and oxidative stress exists, yet whether oxidative stress is a cause or a consequence in the development of this pathology is still unclear (Lee et al., 2010; Macut et al., 2013). Oxidative stress is the result of an imbalance between the production of reactive oxygen species (ROS) and their inactivation by antioxidant mechanisms.

Hyperinsulinemia, a very common feature in PCOS, induces an inflammatory response as evidenced by increased ROS-associated oxidative stress and activation of NF-κB. When ROS induces oxidative stress, NF-κB translocates to the nucleus to promote the transcription of TNFα and IL-6 (Barnes and Karin, 1997). Additionally, chronic inflammation plays a key role in the pathogenesis of PCOS (González, 2012; Sirmans et al., 2012) and is reflected by the presence of C-reactive protein (CRP) in circulation (Kelly et al., 2001). An imbalance among pro- and anti-inflammatory factors could be implicated in impaired endometrial function and infertility associated with PCOS (Amjadi et al., 2018). Chronic inflammation and oxidative stress are closely related. Therefore, it has been proposed a vicious cycle, whereby inflammation induces generation of ROS, while oxidative stress promotes and aggravates inflammation (Duleba and Dokras, 2012). Both factors could induce tissue damage and affect multiple physiological processes such as ovulation, fertilization, implantation, embryo development and pregnancy by altering the function of the ovaries and the uterus (Agarwal et al., 2005).

Peroxisome proliferator-activated receptor gamma (PPARg) has been identified as playing a crucial role in the control of fertility. This receptor is required for the attachment of embryos to the endometrium and for the development and function of the placenta. PPARg also controls the immune response through its ability to inhibit the expression of inflammatory cytokines and to direct the differentiation of immune cells toward anti-inflammatory phenotypes (Minge et al., 2006). Some reports suggest that PPARg regulates inflammatory processes in the endometrium. Moreover, it has been reported that PPARg modulates cyclooxygenase (COX)-2 expression, the limiting enzyme involved in the synthesis of prostaglandins (Zaree et al., 2015).

Prenatal hyperandrogenization (PH) in females leads to the appearance of a PCOS phenotype in adulthood (Abbott et al., 2008; Motta, 2010; Padmanabhan and Veiga-Lopez, 2013; van Houten and Visser, 2014). These prenatally induced-PCOS animal models are usually permanent, due to specific developmental disturbances during the maturation and differentiation of the organs, leading to alterations of their structures and functions (Abbott et al., 2007). Our laboratory has been working in a rat model of PCOS that recreates the endocrine, ovarian, and uterine disturbances of the pathology, thus allowing for the exploration of reproductive and metabolic disorders (Abruzzese et al., 2016; Ferreira et al., 2020; Heber et al., 2019). Using this model, the present work aimed to study the systemic glucose/insulin homeostasis, the oxidant/antioxidant balance, the inflammatory status, and the expression of PPARg in the uterine tissue of prenatally androgenized rats when adult.

2. Materials and Methods

2.1 Experimental animal model and ethics statement

Virgin female rats of the Sprague-Dawley strain were mated with fertile males of the same strain. Three females and one male were housed together under controlled conditions of light (12 h light: 12 h dark) and temperature (23–25°C). Animals received food (Cooperación SRL, Argentina) and water *ad libitum*. Day 0 of pregnancy was defined as the day in which spermatozoa were observed in the vaginal lavages. Between days 16 and 19 of pregnancy, rats were hyperandrogenized as previously described (Abruzzese et al., 2016; Heber et al., 2019). Briefly, pregnant rats (N=15) received subcutaneous injections of 1 mg of free testosterone (Sigma Chemical Co. St. Louis, MO, USA) dissolved in 100 µl of sesame oil (Sigma) on days 16, 17, 18, and 19 of pregnancy, whereas the control group (N=15) received the same number of injections containing only 100 µl of sesame oil used as vehicle. The dose of testosterone administered resulted in circulating testosterone levels similar to those of male rats (Wolf et al., 2002). All the procedures involving animals were conducted in accordance with the 1996 Animal Care and Use Committee of the Consejo Nacional de Investigaciones Científicas y

Técnicas (CONICET). The present study was approved by the Ethics Committee of the Facultad de Medicina, Universidad de Buenos Aires, Argentina.

The treatments described did not modify the spontaneous term labor, the female-to-male offspring ratio, or the number of pups per litter. Under the conditions of our animal facility, spontaneous term labor occurs on day 22 of pregnancy (Abruzzese et al., 2016). Pups were culled from litters to equalize group sizes (ten pups/mother). Female pups were separated from males at 21 days of age, and randomly assigned to each assay, which was carried out with the same number of animals from each randomly selected littermate. The group of female offspring prenatally treated with testosterone was designated as the prenatally hyperandrogenized group or PH group, whereas the offspring of animals receiving vehicle composed the control or C group. The age at vaginal opening did not differ between C and PH groups. These animals showed their vaginal opening around day 33 of life (Abruzzese et al., 2019). Estrous cycles from C and PH groups were monitored daily by vaginal smears beginning at 70 days of age and until decapitation after 90 days. The results of estrous cycle study let us define three experimental groups. The ***control group*** **(C)** had normal cycles (4-6 days), whereas those animals prenatally exposed to androgens showed one of the two following phenotypes: ***ovulatory phenotype*** **(PH ov)** displaying prolonged cycles lasting 7 days or more (going through all stages of the estrous cycle –in order or not-), or ***anovulatory phenotype*** **(PH anov)** with no cycles at all (this group remained arrested at diestrus stage) (Abruzzese et al., 2016; Karim et al., 2003). PH rats displayed a hyperandrogenic state during early puberty and adulthood as evidenced by higher levels of testosterone in the PH groups than in the control group (Abruzzese et al., 2016; Heber et al., 2019). At 90 days (day of euthanasia) the entire PH anov group remained in diestrus; for that reason, and to allow comparison among groups, all animals were killed on the first diestrus after 90 days of age. Female offspring from each experimental set of animals were weighed, anesthetized with carbon dioxide, and killed by decapitation. Trunk blood was collected, and serum was separated and kept at −80°C for further studies. One horn of the uterus was extracted and conserved at -80°C for PCR and Western blot purposes, whereas the other one was fixed in 4% formaldehyde neutral buffered solution for 24

h at 4°C and used for histology purposes. Following paraffin embedding and sectioning (5µm), two sections per sample were stained with hematoxylin and eosin (H&E), whereas subsequent sections were used for immunohistochemical studies.

2.2 Body weight and metabolic parameters

The body weight of all the animals of all the groups was assessed at 21, 28, 38, 45, 60, 75, and 90 days of age. Fasting blood glucose was determined by using Accu-Chek test strips (Roche, Basel, Switzerland) for visual determination in the range of 20–800 mg/100 ml (1–44 mmol/l) (N=10 per group). Fasting insulin levels were measured by an ELISA kit following the manufacturer's instructions (Insulin Human ELISA Kit; Abcam, Cambridge, United Kingdom) (N=10 per group). The intra- and interassay coefficient of variation values for insulin were 10% and 12% respectively. Serum glucose levels were expressed as mg/dl and insulin levels as µIU/ml. The homeostatic model assessment for insulin resistance (HOMA-IR) was calculated according to the formula: fasting insulin (µIU/ml) x fasting glucose (mg/dl)/405 (Matthews et al., 1985).

2.3 Western blot and quantitative analysis

Uterine tissues were lysed and prepared for protein extraction (N=8/group). The lysis solution contained 50 mM Tris-HCl (pH 7.4), 150 mM NaCl (Sigma), 0.5% NP-40 (Sigma), 1 mM PMSF (Sigma), 1 µg/ml pepstatin (Sigma), 2 µg/ml aprotinin (Sigma), 2 µg/ml leupeptin (Sigma), 1 mM DTT (Promega, Madison, WI, USA), 1 mM sodium orthovanadate (Sigma), and 50 mM sodium fluoride (Sigma). This buffer was added to 50 mg of uterine tissue for 30 min at 4°C and subjected to homogenization using a pestle mixer. Uterine lysates were then centrifuged at 14,000 *g* for 20 min at 4°C, and the supernatant was considered the whole cell extract, which was assayed for protein content using the bicinchoninic acid method (BCA; Pierce, Rockford, IL, USA). After boiling for 5 min at 95°C, equal amounts of proteins per group (20 µg) were resolved on 10% or 12% TGX stain-free gels (Bio-Rad Laboratories

GmbH, Munchen, Germany) and transferred onto low fluorescence PVDF membranes (Bio-Rad) for 7 min using the Trans-Blot Turbo Blotting System (Bio-Rad) following the manufacturer´s instructions. The blots were blocked for 1 hour in 5% (w/v) non-fat dry milk in Tris-buffered saline containing 0.1% (v/v) Tween 20 (TBST). After blocking, the membranes were probed overnight at 4°C with the primary antibodies in TBST containing 5% (w/v) non-fat dry milk or 5% (w/v) bovine serum albumin (in the case of phosphorylated proteins). The blots were washed 5 × 5 min in TBST and incubated with HRP-conjugated secondary antibody for 1 hour at room temperature. Blots were washed and developed by chemiluminescence (Clarity Western ECL Substrates, Bio-Rad). Ultraviolet activation of the TGX stain-free gel on a ChemiDoc MP Imaging System (Bio-Rad) was used to control for proper loading. Band densitometry was performed using Image Laboratory Software (Version 6.0, Bio-Rad). When quantified, the intensity of each protein band was normalized to the total protein in individual samples to adjust for unequal loading and transfer (Taylor et al., 2013; Taylor and Posch, 2014; Zhang et al., 2017). The identity of the antibodies used for Western blotting are detailed in Table 1.

Table 1. Antibodies used in the study

Antibody	Brand	Catalog number	WB dilution	IHC dilution
Cyclooxygenase-2	Abcam	Ab15191	1:2000	1:200
GSK-3β	Cell Signaling	12456	1:1000	
Phospho-GSK-3β	Cell Signaling	9336	1:1000	
NF-κB	Cell Signaling	8242	1:1000	
PPAR gamma	Abcam	Ab209350	1:1000	1:100
Goat Anti-Rabbit IgG -HRP Conj.	Bio-Rad	1706515	1:10000	
Goat Anti-Mouse IgG – HRP Conj.	Jackson	115-035-003	1:8000	

Table 1. List of antibodies and dilution used for western blotting (WB) and immunohistochemistry (IHC) purposes.

2.4 Immunohistochemical analysis

Paraffin sections (N=5/group) were deparaffinized and rehydrated through a graded alcohol *series followed by antigen retrieval in 10 mM sodium citrate buffer, pH 6.0 for 40 min with steaming (IHC WORLD, Woodstock, MD, USA). Slides were treated with 0.5% Triton X-100 to allow permeabilization. Thereafter, slides were blocked with 5% normal horse serum (NHS) (Vector Labs, Burlingame, CA, USA)* for 20 minutes at room temperature. The primary antibodies (see list and concentrations on Table 1) were diluted in NHS and incubated overnight at 4°C or for 1 hour at room temperature in a humidified chamber. Thereafter, the sections were incubated with 3% hydrogen peroxide to remove endogenous peroxidase activity. After being washed with phosphate-buffered saline containing 0.1% (v/v) Tween 20 (PBST), and phosphate-buffered saline (PBS), the samples were incubated for 30 minutes at room temperature with the secondary antibodies identified in Table 1. Sections were visualized with 3,3-diaminobenzidine *tetrahydrochloride* (Vector Labs). Negative controls were performed, following the same protocol, except that the tissue was not incubated with a primary antibody. Positive tissue controls were performed using cancer cell lines that are known to express the proteins of interest (data not shown). Slides were viewed on a microscope (Amscope MU1000) and photomicrographed using AmScope Software 3.7 (United Scope LLC, Irvine, CA, USA)

2.5 Quantification of mRNA levels by real-time PCR

We assessed the mRNA expression of *PPARg*, *COX-2*, *NcOR*, *Cu-SOD*, *TNFa*, *IL-10* and *NF-κB*. All mRNA levels were evaluated by real-time PCR analysis (N=6/group). Briefly, total mRNA from uterine tissue was extracted using RNAzol RT (MRC gene, Molecular Research Center, Cincinnati, OH, USA), following the manufacturer´s instructions. cDNA was synthesized from 1 µg mRNA using random primer hexamers (Invitrogen-Life Technologies, Buenos Aires, Argentina). Real-time PCR analysis was performed from this cDNA (2.5µL) in 10 µl reaction buffer containing 20 mM dNTPs mix, GoTaq Polymerase (Promega), Eva Green 20x (Biotium Hayward, CA, USA), and gene-specific primers in a total volume of 12.5 µl. The qPCR conditions started with a denaturation step at 95°C for 5 min and followed by up to 50 cycles of denaturation (95°C), annealing (see temperature for each primer in Table 2) and

primer extension (72 °C). The amplified products were quantified by fluorescence using the Rotor-Gene 6000 (Corbett Life Science, Sydney, Australia), and mRNA abundance was normalized to the amount of 60s Ribosomal protein L32 (L32). L32 was validated as a reference gene as the variance between treatments did not differ. Gene expression was quantified using the $2^{-\Delta\Delta Ct}$ method (Livak and Schmittgen, 2001). Results are expressed as a fold value of the controls.

Table 2. Primers used in the study

Gene	Primer sequences	Temperature of melting (°C)
L32 F	TGGTCCACAATGTCAAGG	58
L32 R	CAAAACAGGCACACAAGC	
Ncor F	TATCGGAGCCATCTTCCCAC	60
Ncor R	ACTTGGGTATCCTGGGGTTG	
Cusod F	GTCGTCTCCTTGCTTTTTGC	62
Cusod R	TGCTCGCCTTCAGTTAATCC	
Tnfα F	GATCGGTCCCAACAAGGAGG	62
Tnfα R	CTTGGTGGTTTGCTACGACG	
Il10 F	TGAAAAATTGAACCACCCGGC	62
Il10 R	CCAAGGAGTTGCTCCCGTTAG	
Nf-κb F	GAAGAGGATGTGGGGTTTCA	62
Nf-κb R	CTGAGCATGAAGGTGGATGA	
Pparg F	TTTTCAAGGGTGCCAGTTTC	60
Pparg R	GAGGCCAGCATGGTGTAGAT	
Cox-2 F	ATCCTGCCAGCCAGCTCCACCG	62
Cox-2 R	TGGTCAAATCCTGTGCTCATACAT	

Table 2. List of primers used in the real-time PCR. F, forward sequence; R, reverse sequence.

2.6 Oxidative stress-related parameters

2.6.1 Lipid peroxidation

The amount of malondialdehyde (MDA) formed from the breakdown of polyunsaturated fatty acids may be taken as an index of peroxidation reaction. The method used in the present study was previously described (Motta et al., 2001), and quantifies MDA as the product of lipid

peroxidation that reacts with trichloracetic acid–thiobarbituric acid–HCl (15% (w/v); 0.375% (w/v) and 0.25M, respectively), yielding a red compound that absorbs at 535 nm. Homogenates of uterine tissue (N=15/group) were treated with trichloroacetic acid–thiobarbituric acid–HCl and heated for 15 min in a boiling water bath. After cooling, the flocculent precipitate was removed by centrifugation at 1000 *g* for 10 min. The absorbance of samples was determined at 535 nm. The content of thiobarbituric acid reactants was expressed as nM MDA formed/mg protein.

2.6.2 Glutathione (GSH) content

The antioxidant metabolite GSH was quantified as previously described (Elia, 2006). The reduced form of GSH comprises the bulk of cellular protein sulfhydryl groups. Thus, measurement of acid soluble thiol is used to estimate the GSH content in tissue extracts. Briefly, one uterus per point was homogenized in homogenization buffer (EDTA (1 mM), KCl (150 mM), beta-mercaptoethanol (1 mM), trizma base (20 mM), and sacarose (500 mM), pH=7.6), and centrifuged at 800 *g* for 10 minutes at 4°C (N=15/group). Then, supernatants (50 µl/point) were incubated with 800 µl of 1.5 M Tris buffer (pH 7.4) containing 50 µl of 5.10^{-3} M NADPH and 6 IU of GSH reductase. The reaction involves the enzymatic reduction of the oxidized form (GSSG) to GSH. When Ellman's reagent (a sulfhydryl reagent 5,5-dithiobis-2 nitrobenzoic acid (Sigma) is added to the incubation medium, the chromophoric product resulting from this reaction develops a molar absorption at 412 nm that is linear beyond 6 min; thereafter the reaction remains constant. Results are expressed as µM GSH/mg protein.

2.7 Serum C-reactive protein levels determination

Quantitative determination of serum C-reactive protein (CRP) was analyzed using an immunoturbidimetric method (#1683267, Wiener Lab, Argentina) following the manufacturer's instructions (N=15 per group). The CRP reacts with the specific antibody producing insoluble immune complexes. The turbidity caused by these immune complexes is proportional to the concentration of CRP in the sample. The complexes were measured spectrophotometrically at

340 nm at 37°C. The intra- and interassay coefficient of variation values were 2.4% and 6.0%, respectively.

2.8 Statistical analysis

Statistical analyses were performed to test the number of samples needed for each experiment using Infostat Software (Di Rienzo et al., 2011). The same software was used to test the normality of data (Shapiro-Wilks test) and homoscedasticity (Levene's test). Results are presented as the means ± S.E.M. Statistical analyses were performed using GraphPad Instat® software (GraphPad Software, San Diego, CA, USA). For normally distributed data, differences between groups were analyzed by one-way ANOVA followed by Tukey's multiple comparison test.

3. Results

3.1 Prenatal androgen excess induces insulin resistance without altering uterine weight

Insulin resistance homeostasis and growth curve were evaluated to determine, respectively, if prenatal androgen excess impairs glucose/insulin homeostasis and gain weight during adulthood. Results showed that basal glucose levels were significantly increased in a phenotype dependent manner in the PH groups (Fig.1 A). Moreover, insulin levels were increased in both PH groups with respect to the control group (Fig.1 B). The homeostatic model of assessment for insulin resistance index (HOMA-IR) was increased in the PH groups if compared with the control group (Fig.1 C). Prenatal hyperandrogenization did not affect the body weight from prepubertal to adult age evaluated through a weight curve during 90 days (Fig.1 D). Moreover, as a measurement of the relation between uterine growth and body weight, the ratio between these factors was analyzed, and showed no differences between groups (Fig.1 E).

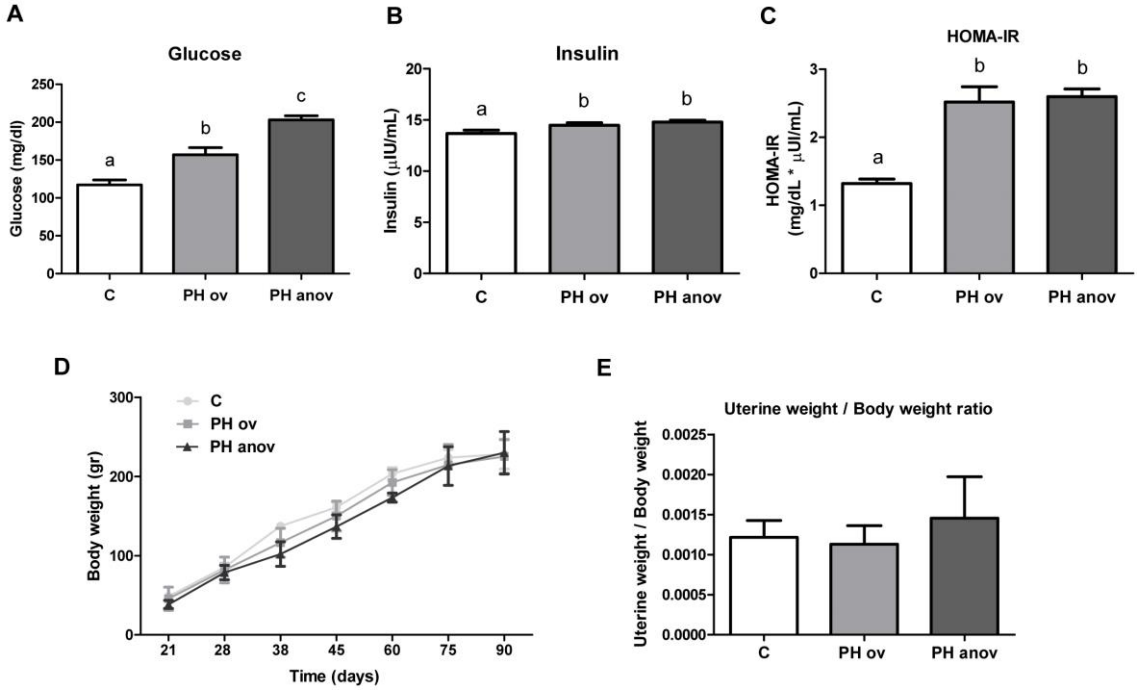

Figure 1. Effects of prenatal hyperandrogenization on body growth curve and metabolic status. Metabolic features evaluated in the female offspring of prenatally hyperandrogenized (PH) and control (C) groups. Basal glucose levels **(A)**, basal insulin levels **(B)** and HOMA-IR index **(C)** (N = 10/group); the curve represents the mean growth rates of the C and PH groups **(D)**; uterine weight: body weight ratio **(E)**. Each column represents the mean ± S.E.M. Different letters represent statistical significance among the groups, $p<0.05$.

3.2 Prenatal androgen excess alters the expression of PPARg in the uterine tissue

Due to its important role in reproduction, we evaluated the gene and protein expression of PPARg in the uterine tissue. Immunohistochemistry showed that the PPARg expression is confined to the glandular (Fig.2 A-C) and luminal epithelium (Fig.2 D-F) in all the groups studied. Although protein levels of PPARg showed no differences among the groups (Fig.2 G), a decrease in gene expression of PPARg was found in the PH anov group (Fig.2 H, J). Moreover, the nuclear co-repressor NcOR, which represses PPARg, was found to be decreased in the PH anov group (Fig.2 I).

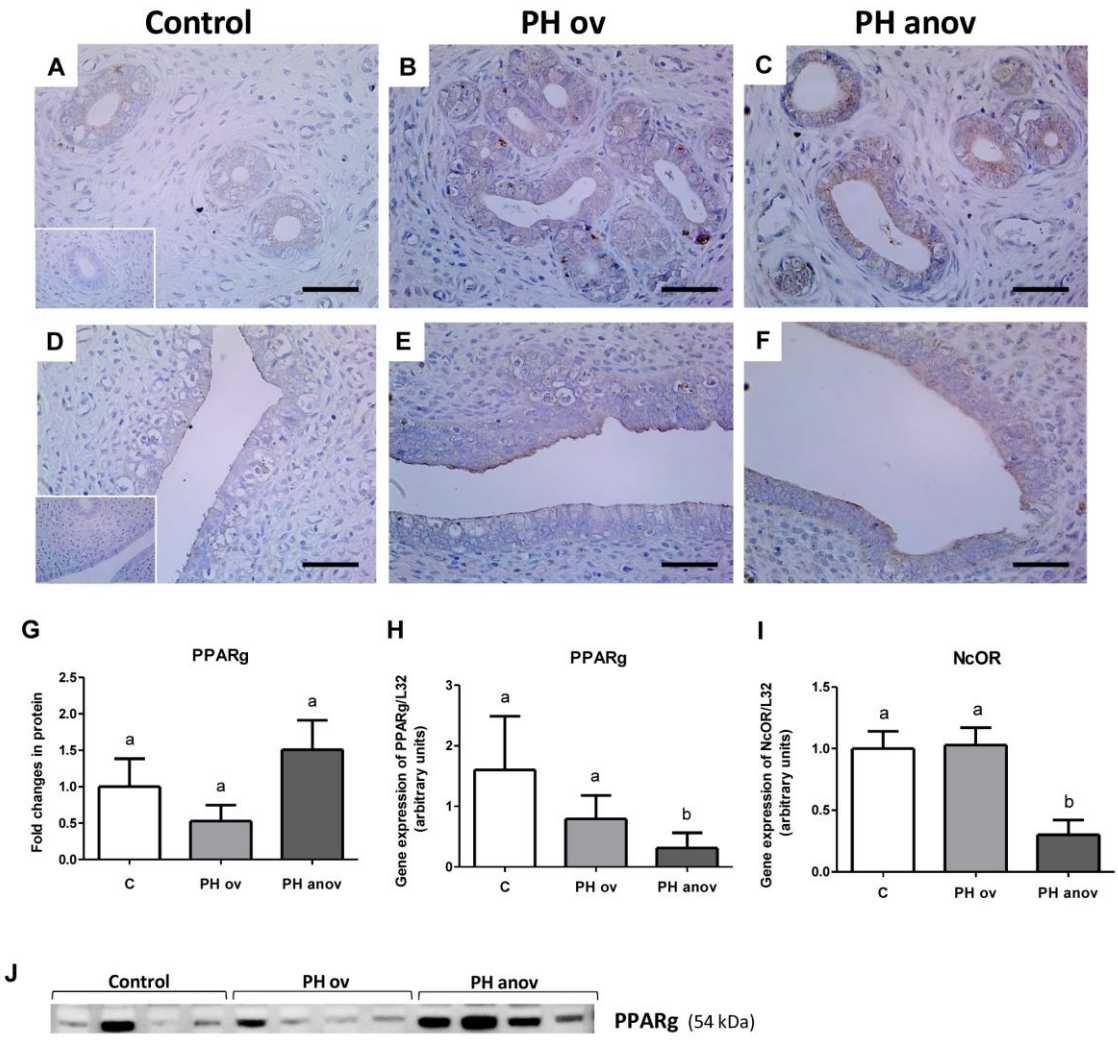

Figure 2. Effects of prenatal hyperandrogenization on PPARg expression. PPARg uterine expression was evaluated in the prenatally hyperandrogenized (PH) and control (C) groups. Immunohistochemical detection of PPARg in paraffin embedded uterine tissue sections of rats in diestrus, from control **(A, D)**, PH ov **(B, E)**, or PH anov **(C, F)** groups. Scale bars are indicated in the photomicrographs and represents 50 µm **(A-F)**. As a negative control, the primary antibody was omitted (insert in A, D) (N = 5/group). Results of Western blotting for PPARg **(G, J)**; equal amounts of uterine proteins were loaded in each lane (N = 8/group), mRNA expression of *PPARg* **(H)** and *NcOR* **(I)** both relative to *L32* (N = 6/group). Each column represents the mean ± S.E.M. Different letters represent statistical significance among the groups, $p<0.05$.

3.3 Prenatal androgen excess induces a pro-inflammatory state in the uterine tissue

We studied the expression of pro-inflammatory (COX-2, TNFα, CRP) and anti-inflammatory markers (IL-10), and of NF-κB as a regulator of the expression of inflammatory genes. Positive COX-2 staining was found mainly in the glandular and luminal epithelium of the uterine tissue (Fig.3 A-F). When assessed by western blotting, COX-2 protein expression was found to be increased in the PH groups (Fig.3 G, I) when compared to the C group. Moreover, mRNA levels of COX-2 were increased in a phenotype dependent manner in both PH groups (Fig.3 H). Increased expression of NF-κB protein was found only in the PH ov group (Fig.4 A, B); however, no differences were found in the NF-κB mRNA levels among all groups studied (Fig.4 C). Furthermore, mRNA levels of TNFα were analyzed but no differences were found between groups (Fig.4 D). On the other hand, as an anti-inflammatory marker, we evaluated the mRNA expression of IL-10, and we found that only the PH ov group presents significantly increased IL-10 mRNA levels (Fig.4 E). As a systemic inflammatory marker, serum levels of CRP were found to be increased in the PH anov group when compared to the control group (Fig.4 F).

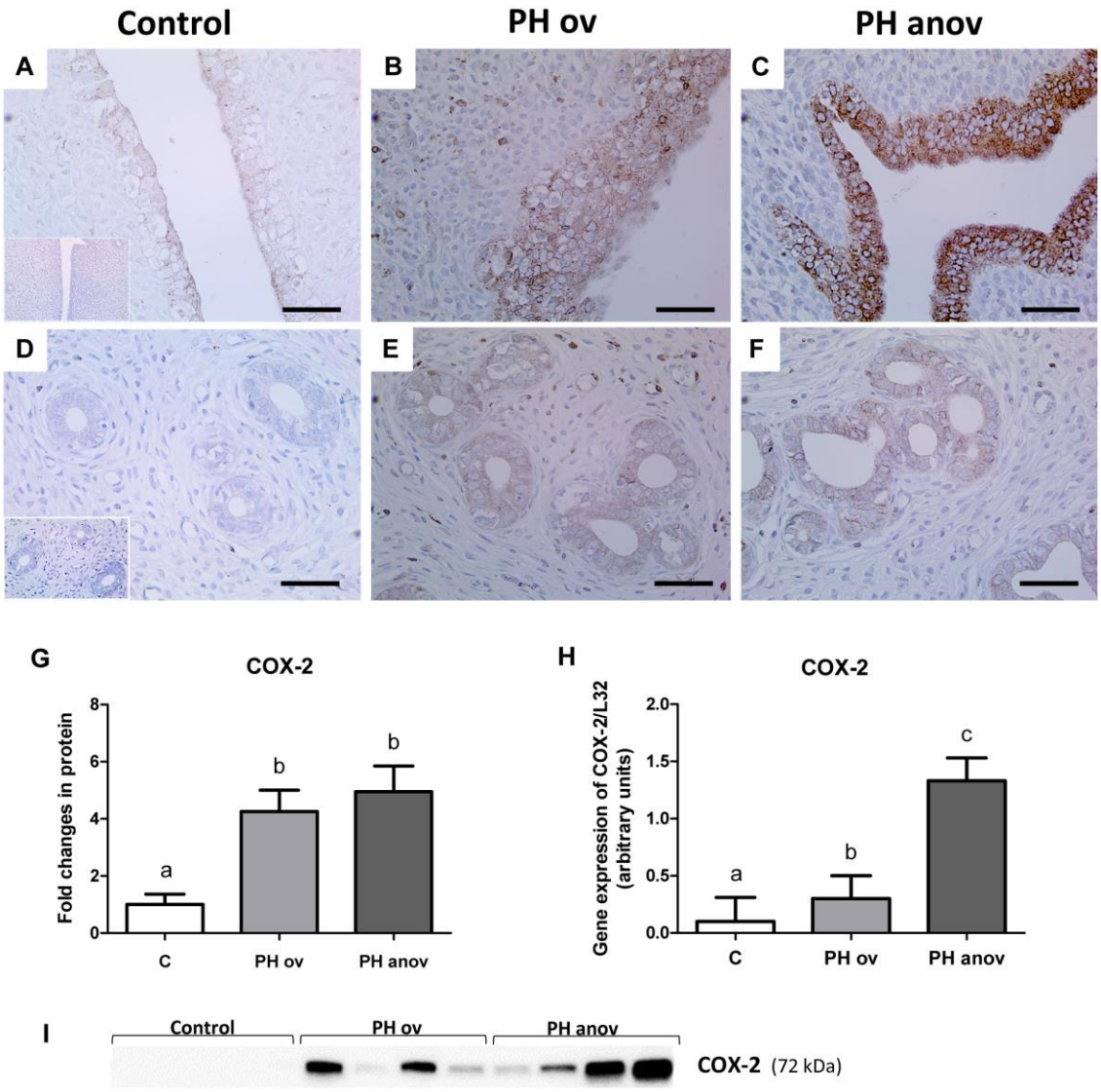

Figure 3. Effects of prenatal hyperandrogenization on COX-2 expression. COX-2 was evaluated in the uterus of prenatally hyperandrogenized (PH) and control (C) groups. Immunohistochemical detection of COX-2 in paraffin embedded uterine tissue sections of rats in diestrus, from control **(A, D)**, PH ov **(B, E)**, or PH anov **(C, F)** groups. Scale bars are indicated in the photomicrographs and represents 50 µm **(A-F)**. As a negative control, the primary antibody was omitted (insert in A, D) (N = 5/group). Results of Western blotting for COX-2 **(G, I),** equal amounts of uterine proteins were loaded in each lane (N = 8/group); mRNA expression of *COX-2* **(H)** relative to *L32* (N = 6/group). Each column represents the mean ± S.E.M. Different letters represent statistical significance among the groups, $p<0.05$.

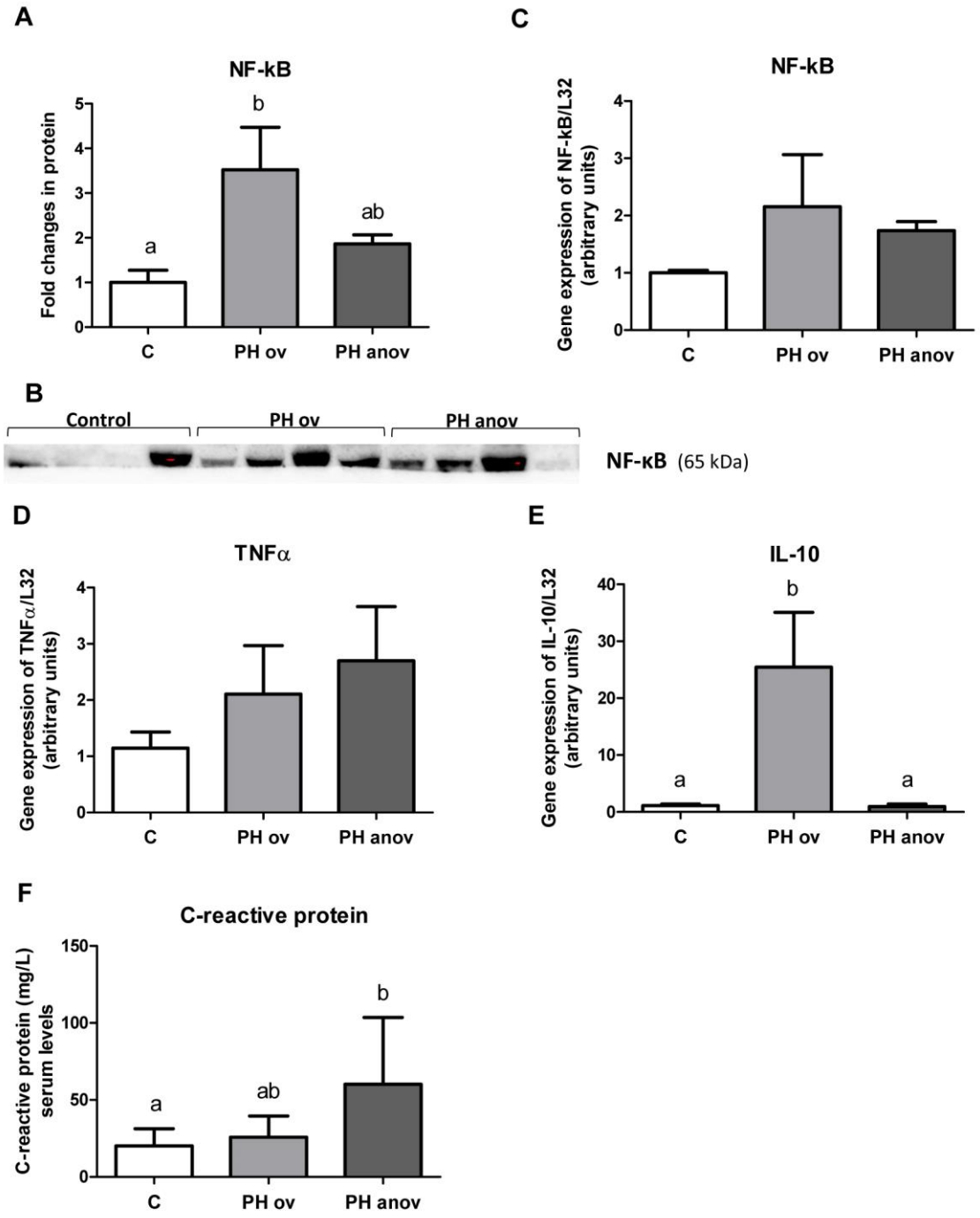

Figure 4. Effects of prenatal hyperandrogenization on inflammation markers. Inflammation markers were evaluated in the uterus of prenatally hyperandrogenized (PH) and control (C) groups. Results of Western blotting for NF-κB **(A, B)** [equal amounts of uterine proteins were loaded in each lane (N = 8/group)], and mRNA expression of *NF-κB* **(C)** were studied; mRNA expression of *TNFα* **(D)** relative to *L32*; mRNA expression of *IL-10* **(E)** relative to *L32* (N = 6/group). Serum levels of C-reactive protein (CRP) **(F)** (N = 10/group). Each

column represents the mean ± S.E.M. Different letters represent statistical significance among the groups, $p<0.05$.

3.4 Prenatal androgen excess creates an unbalanced oxidative status

The oxidant–antioxidant balance in the uterine tissue was evaluated. The lipid peroxidation index was assessed by using the thiobarbituric acid method (TBARs) through the evaluation of malondialdehyde (MDA); results revealed an increased lipid peroxidation index in the PH anov group (Fig. 5A). Whereas TBARs showed a tendency to increase also in the PH ov group, such increase was not statistically significant (Fig.5 A). Additionally, the content of the antioxidant glutathione was found increased in the PH anov group (Fig.5 B). On the other hand, both PH groups showed decreased levels of the mRNA encoding for Cu-SOD, another antioxidant enzyme (Zuo et al., 2016) (Fig.5 C).

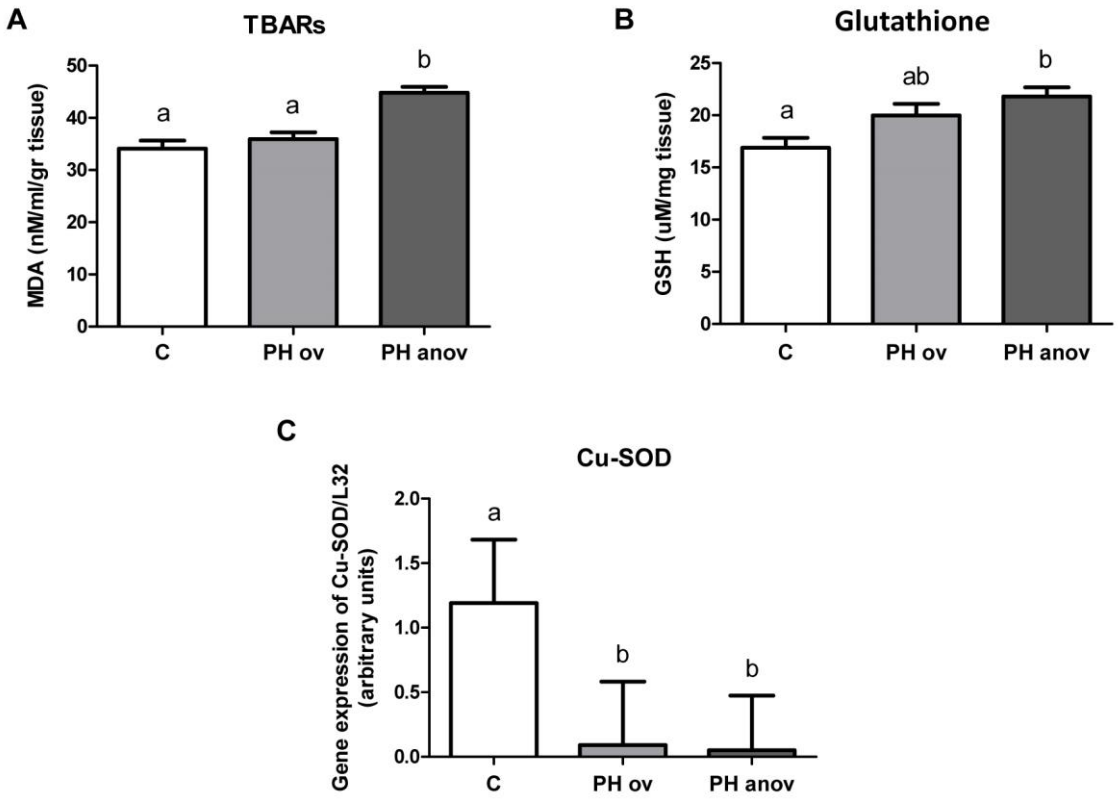

Figure 5. Effects of prenatal hyperandrogenization on uterine oxidant/antioxidant balance. The oxidant–antioxidant balance in the uterine tissue was evaluated in the prenatally hyperandrogenized (PH) and control (C) groups by analyzing the lipid peroxidation index using

the thiobarbituric acid method (TBARs) through evaluation of malondialdehyde (MDA) **(A)** and the content of the antioxidant glutathione (N = 15/group) **(B)**. mRNA expression of *Cu-SOD* **(C)** relative to *L32* (N = 6/group). Each column represents the mean ± S.E.M. Different letters represent statistical significance among the groups, *p<0.05.*

3.5 Prenatal androgen excess induces GSK-3β phosphorylation in the uterine tissue

GSK-3β has numerous functions in the cells; the most important are related with glucose homeostasis and NF-κB signaling (Lee and Kim, 2007). Western blot results revealed that the expression of the total form of GSK-3β (Fig.6 A, C) and the phosphorylated form of GSK-3β on Ser 9 (Fig.6 B, C) were increased in both PH groups when compared to the controls.

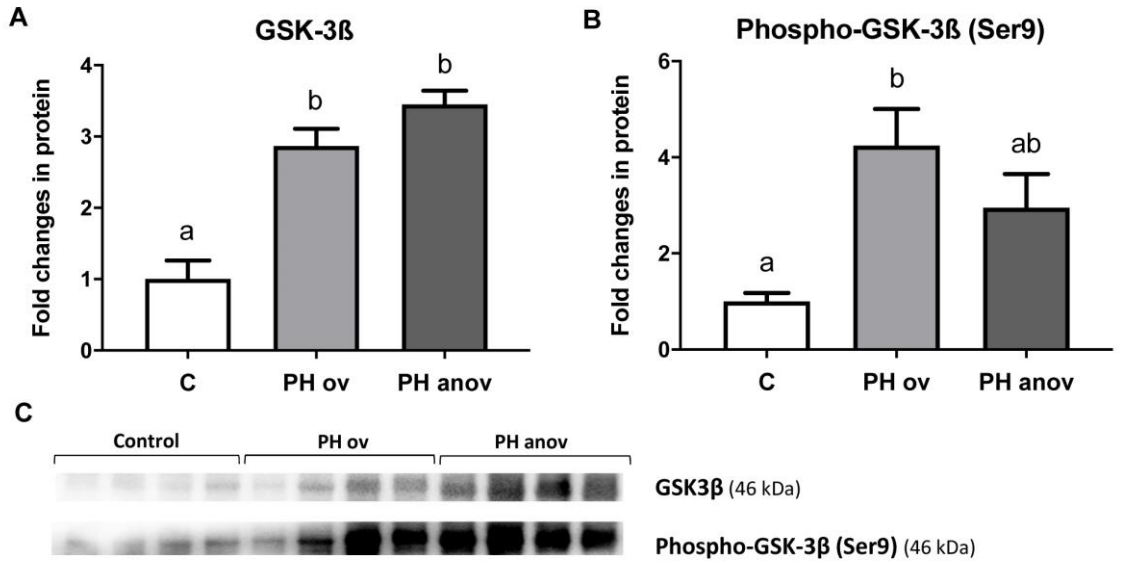

Figure 6. Effects of prenatal hyperandrogenization on GSK-3β expression. GSK-3β total and phosphorylated form were evaluated in the prenatally hyperandrogenized (PH) and control (C) groups. Results of Western blotting for GSK-3β **(A, C)** and phospho-GSK-3β (Ser9) **(B, C)**; equal amounts of uterine proteins were loaded in each lane (N = 8/group). Each column represents the mean ± S.E.M. Different letters represent statistical significance among the groups, *p<0.05.*

4. Discussion

In this study, we used our rat model that mimics PCOS features through prenatal testosterone exposure. Female offspring showed two phenotypes, ovulatory and anovulatory confirming our previous reports (Abruzzese et al., 2019; Ferreira et al., 2020).

Oxidative stress and inflammation have been related to the pathogenesis of PCOS (Escobar-Morreale et al., 2011; Zhao et al., 2015). Moreover, it has been described that PCOS patients present a pro-inflammatory state that could be aggravated by the presence of insulin resistance (Palomba et al., 2014). Furthermore, as PPARg was reported to be a modulator of proliferation, inflammation, and cell differentiation processes in the uterus (Brooks et al., 2015; Nickkho-Amiry et al., 2012), it might play an important role in the reproductive function. Therefore, considering PPARg as an energy-metabolic sensor, it could be used as a good indicator of the uterine inflammatory and redox state, particularly during pregnancy (Schaiff et al., 2006). Under physiological conditions, the PPAR system regulates uterine function; consequently, we aimed to evaluate how altered PPARg is in the uterus under the pathological condition of our PCOS model. Results show altered expressions of PPARg and NcOR in the PH anov phenotype, suggesting a possible dysregulation of the downstream pathways that PPARg control. The results are in accordance with previous reports from our laboratory in which prenatal hyperandrogenization was induced with a higher dose of testosterone (Ferreira et al., 2019). However, previously in our laboratory, opposite results were found at the level of the ovaries (Amalfi et al., 2012). This discrepancy could be explained due to the different amount of testosterone used, or because of organ specificity. Furthermore, other authors have reported a decrease in PPARg expression in endometrial cancer and in other tumor cell types (Knapp et al., 2012).

PPARg regulates the expression and activity of COX-2 (Sheldrick et al., 2007). This can be explained considering the existence of a direct interaction between PPARs and prostaglandins due to the presence of a PPAR response element in the promoter of the COX-2 gene (Knopfová and šMarda, 2010; Meade et al., 1999). In the present work, our results revealed that PH induces a pro-inflammatory state in the uterine tissue evidenced by an increase in the uterine expression

of COX-2. Previously, we demonstrated that under this model of prenatal androgen excess, the luminal epithelium of the endometrium becomes hyperplastic (Ferreira et al., 2020). Taken together, these results suggest that the deregulation of tissue homeostasis triggers a pro-inflammatory state in the luminal epithelium of the uterine tissue. Moreover, alterations in the expression of COX-2 and PPARg have been found in endometriosis and in different types of cancer (Adelizzi, 1999; Sobolewski et al., 2010), but have not yet been elucidated in the endometrium of animals exposed to prenatal androgen excess. Several studies have reported an inverse correlation between PPARg and COX-2 levels in different types of cancers (Badawi and Badr, 2003; Gustafsson et al., 2007; Knopfová and šMarda, 2010; Konstantinopoulos et al., 2007); we found a similar trend in the uterine tissue of the PH anov group. This is interesting as the weaker the expression of PPARg, the higher the level of COX-2 / PGE-2, which could favor tumor development and progression (Badawi and Badr, 2003; Sasaki et al., 2002).

Our results also showed that the PH anov group presents an elevated systemic inflammatory status as depicted by elevated CRP, which is considered a biomarker of low-grade chronic inflammation in women with PCOS (Repaci et al., 2011). Our data are in agreement with other investigations that have reported significantly increased CRP levels in patients with PCOS (Bannigida et al., 2018; Blumenfeld, 2019; Boulman et al., 2004).

Our animal model of prenatal androgen excess let us recreate numerous PCOS features, among them oxidative stress, which is considered a contributing factor in triggering the condition. We also found that PH increased lipid peroxidation in the anovulatory phenotype; as a response, the antioxidant mediator GSH increased, suggesting a compensatory mechanism against the hyper-oxidative state. In contrast, another protective mechanism against oxidative stress mediated by Cu-SOD was depleted in the PH groups. As a summary, studies indicate that oxidative stress is increased in PCOS patients when compared to patients without PCOS (Escobar-Morreale et al., 2011; Murri et al., 2013). It has also been shown that oxidative stress significantly correlates with obesity, hyperandrogenism, insulin resistance, and chronic inflammation (Lu et al., 2018).

Insulin resistance induces oxidative stress because hyperglycemia and high levels of free fatty acids lead to the production of ROS (Bloch-Damti and Bashan, 2005; Lee et al., 2010). Thus,

insulin resistance found in PH groups could explain the pro-oxidant status found in these animals. Moreover, other authors have demonstrated that ROS and pro-inflammatory factors, produced under oxidative stress, could induce insulin resistance mainly through the PI3K-Akt pathway by activating NF-κB and JUNK, likely via GSK-3β (Kamata et al., 2005; Keane et al., 2015). In agreement, PH groups present increased Ser 9 phosphorylation of GSK-3β, suggesting an activation of AKT (Heber et al., 2019).

In the current work, we found elevated levels of glucose and insulin in the circulation of the PH groups. Hyperinsulinemia together with oxidative stress may promote cell proliferation and genetic instability due to DNA damage leading to malignant transformation and the development of cancer in a context of PCOS (Papaioannou and Tzafettas, 2010). Also, it has been demonstrated that oxidative stress is associated with metabolic disorders that could interfere in the physiology of PCOS, and are potential inducers of the characteristic associated features of the pathology (Di˙ncer et al., 2005; González et al., 2009). Moreover, it was reported in patients with PCOS that oxidative stress and inflammation markers correlate positively with androgen levels (González et al., 2005; Yang et al., 2011; Yilmaz et al., 2005).

It is important to point out that mRNAs does not always directly reflects what happen at the protein level. Modifications to mRNA could affect their stability and its levels, affecting their translational efficiency. Moreover, miRNAs function to control translation efficiencies, which may be why some RNAs may not be translated. In contrast, others are translated more efficiently. Another critical factor is the protein stability, which also could be affected by a post-translational modification. These issues could explain in some part the different results between mRNA and protein levels obtained in the present study.

In conclusion, this study demonstrated that prenatal hyperandrogenization in an animal model which mimics metabolic, ovarian, and uterine features of PCOS. We recognize the limitations of animal models; however, the findings presented in this study could help to elucidate the extent of prenatal hyperandrogenization misbalances, especially in the uterus, which is a very relevant reproductive organ. Prenatal exposure to testosterone lead to the development of systemic insulin resistance, and uterine oxidative stress and inflammation. All these finding are

known features that contribute to the pathogenesis of PCOS and may likely increase the risk of malignant transformation in the uterus.

Funding

This research was supported by Agencia Nacional de Ciencia y Técnica (ABM Grant number 557/2012; 689/2013; 632/2016), and grant number 35635 from the Canada Foundation for Innovation (CMT). Silvana Ferreira was the recipient of a scholarship from the Emerging Leaders in the Americas Program (ELAP), provided with the support of the Government of Canada. Alicia Goyeneche was supported by a Hartland Molson Fellowship from the Research Institute, McGill University Health Centre.

Author contributions

S.R.F: Formal analysis, Investigation, Methodology. A.A.G, M.F.H, M.J.F, and G.A.A: Investigation, Methodology. C.M.T and A.B.M: Conceptualization, Data curation, Formal analysis, Funding acquisition, Project administration, Resources, Supervision, Validation, Visualization, Writing -original draft, Writing - review & editing.

Declaration of competing interest

The author(s) declared no potential conflicts of interest with respect to the research, authorship, and/or publication of this article.

Acknowledgments

We want to thank Enzo Cuba and Marcela Marquez for their technical support in the animal care.

References

- Abbott, D.H., Dumesic, D.A., Levine, J.E., Dunaif, A., Padmanabhan, V., 2007. Animal Models and Fetal Programming of the Polycystic Ovary Syndrome, in: Azziz, R.,

Nestler, J.E., Dewailly, D. (Eds.), Androgen Excess Disorders in Women: Polycystic Ovary Syndrome and Other Disorders, Contemporary Endocrinology. Humana Press, Totowa, NJ, pp. 259–272. https://doi.org/10.1007/978-1-59745-179-6_23

- Abbott, D.H., Zhou, R., Bird, I.M., Dumesic, D.A., Conley, A.J., 2008. Fetal programming of adrenal androgen excess: lessons from a nonhuman primate model of polycystic ovary syndrome. Endocr Dev 13, 145–158. https://doi.org/10.1159/000134831
- Abruzzese, G.A., Heber, M.F., Campo Verde Arbocco, F., Ferreira, S.R., Motta, A.B., 2019. Fetal programming by androgen excess in rats affects ovarian fuel sensors and steroidogenesis. J Dev Orig Health Dis 1–14. https://doi.org/10.1017/S2040174419000126
- Abruzzese, G.A., Heber, M.F., Ferreira, S.R., Velez, L.M., Reynoso, R., Pignataro, O.P., Motta, A.B., 2016. Prenatal hyperandrogenism induces alterations that affect liver lipid metabolism. J. Endocrinol. 230, 67–79. https://doi.org/10.1530/JOE-15-0471
- Adelizzi, R.A., 1999. COX-1 and COX-2 in health and disease. J Am Osteopath Assoc 99, S7-12.
- Agarwal, A., Gupta, S., Sharma, R.K., 2005. Role of oxidative stress in female reproduction. Reprod. Biol. Endocrinol. 3, 28. https://doi.org/10.1186/1477-7827-3-28
- Amalfi, S., Velez, L.M., Heber, M.F., Vighi, S., Ferreira, S.R., Orozco, A.V., Pignataro, O., Motta, A.B., 2012. Prenatal Hyperandrogenization Induces Metabolic and Endocrine Alterations Which Depend on the Levels of Testosterone Exposure. PLoS ONE 7, e37658. https://doi.org/10.1371/journal.pone.0037658
- Amjadi, F., Mehdizadeh, M., Ashrafi, M., Nasrabadi, D., Taleahmad, S., Mirzaei, M., Gupta, V., Salekdeh, G.H., Aflatoonian, R., 2018. Distinct changes in the proteome profile of endometrial tissues in polycystic ovary syndrome compared with healthy fertile women. Reproductive BioMedicine Online 37, 184–200. https://doi.org/10.1016/j.rbmo.2018.04.043
- Badawi, A.F., Badr, M.Z., 2003. Expression of cyclooxygenase-2 and peroxisome proliferator-activated receptor-gamma and levels of prostaglandin E2 and 15-deoxy-delta12,14-prostaglandin J2 in human breast cancer and metastasis. Int. J. Cancer 103, 84–90. https://doi.org/10.1002/ijc.10770
- Badawy, A., Elnashar, A., 2011. Treatment options for polycystic ovary syndrome. Int J Womens Health 3, 25–35. https://doi.org/10.2147/IJWH.S11304
- Bannigida, D.M., Shivananda Nayak, B., Vijayaraghavan, R., 2018. Insulin resistance and oxidative marker in women with PCOS. Archives of Physiology and Biochemistry 1–4. https://doi.org/10.1080/13813455.2018.1499120
- Barnes, P.J., Karin, M., 1997. Nuclear factor-kappaB: a pivotal transcription factor in chronic inflammatory diseases. N. Engl. J. Med. 336, 1066–1071. https://doi.org/10.1056/NEJM199704103361506
- Bloch-Damti, A., Bashan, N., 2005. Proposed Mechanisms for the Induction of Insulin Resistance by Oxidative Stress. Antioxidants & Redox Signaling 7, 1553–1567. https://doi.org/10.1089/ars.2005.7.1553
- Blumenfeld, Z., 2019. The Possible Practical Implication of High CRP Levels in PCOS. Clin Med Insights Reprod Health 13. https://doi.org/10.1177/1179558119861936
- Boulman, N., Levy, Y., Leiba, R., Shachar, S., Linn, R., Zinder, O., Blumenfeld, Z., 2004. Increased C-reactive protein levels in the polycystic ovary syndrome: a marker of cardiovascular disease. J. Clin. Endocrinol. Metab. 89, 2160–2165. https://doi.org/10.1210/jc.2003-031096
- Brooks, K.E., Burns, G.W., Spencer, T.E., 2015. Peroxisome Proliferator Activator Receptor Gamma (PPARG) Regulates Conceptus Elongation in Sheep. Biol Reprod 92. https://doi.org/10.1095/biolreprod.114.123877
- Di˙ncer, Y., Akcay, T., Erdem, T., Saygi˙li˙, E.I., Gundogdu, S., 2005. DNA damage, DNA susceptibility to oxidation and glutathione level in women with polycystic ovary syndrome. Scandinavian Journal of Clinical and Laboratory Investigation 65, 721–728.

https://doi.org/10.1080/00365510500375263

- Di Rienzo, J.A., Casanoves, F., Balzarini, M.G., González, L., Tablada, M., Robledo, y C., 2011. InfoStat versión 2011. Grupo InfoStat, FCA, Universidad Nacional de Córdoba, Argentina. URL http://www. infostat. com. ar 8, 195–199.
- Duleba, A.J., Dokras, A., 2012. Is PCOS an inflammatory process? Fertil. Steril. 97, 7–12. https://doi.org/10.1016/j.fertnstert.2011.11.023
- Elia, E., 2006. The mechanisms involved in the action of metformin in regulating ovarian function in hyperandrogenized mice. Molecular Human Reproduction 12, 475–481. https://doi.org/10.1093/molehr/gal057
- Elnashar, A.M., 2011. The role of metformin in ovulation induction: Current status. Middle East Fertility Society Journal 16, 175–181. https://doi.org/10.1016/j.mefs.2010.10.003
- Escobar-Morreale, H.F., Luque-Ramírez, M., González, F., 2011. Circulating inflammatory markers in polycystic ovary syndrome: a systematic review and metaanalysis. Fertil. Steril. 95, 1048-1058.e1–2. https://doi.org/10.1016/j.fertnstert.2010.11.036
- Ferreira, S.R., Goyeneche, A.A., Heber, M.F., Abruzzese, G.A., Telleria, C.M., Motta, A.B., 2020. Prenatally androgenized female rats develop uterine hyperplasia when adult. Molecular and Cellular Endocrinology 499, 110610. https://doi.org/10.1016/j.mce.2019.110610
- Ferreira, S.R., Vélez, L.M., F Heber, M., Abruzzese, G.A., Motta, A.B., 2019. Prenatal androgen excess alters the uterine peroxisome proliferator-activated receptor (PPAR) system. Reprod. Fertil. Dev. https://doi.org/10.1071/RD18432
- González, F., 2012. Inflammation in Polycystic Ovary Syndrome: underpinning of insulin resistance and ovarian dysfunction. Steroids 77, 300–305. https://doi.org/10.1016/j.steroids.2011.12.003
- González, F., Minium, J., Rote, N.S., Kirwan, J.P., 2005. Hyperglycemia Alters Tumor Necrosis Factor-α Release from Mononuclear Cells in Women with Polycystic Ovary Syndrome. None 90, 5336–5342. https://doi.org/10.1210/jc.2005-0694
- González, F., Rote, N.S., Minium, J., Kirwan, J.P., 2009. Evidence of proatherogenic inflammation in polycystic ovary syndrome. Metabolism - Clinical and Experimental 58, 954–962. https://doi.org/10.1016/j.metabol.2009.02.022
- Gustafsson, A., Hansson, E., Kressner, U., Nordgren, S., Andersson, M., Wang, W., Lönnroth, C., Lundholm, K., 2007. EP1-4 subtype, COX and PPAR gamma receptor expression in colorectal cancer in prediction of disease-specific mortality. Int. J. Cancer 121, 232–240. https://doi.org/10.1002/ijc.22582
- Heber, M.F., Ferreira, S.R., Abruzzese, G.A., Raices, T., Pignataro, O.P., Vega, M., Motta, A.B., 2019. Metformin improves ovarian insulin signaling alterations caused by fetal programming. J. Endocrinol. https://doi.org/10.1530/JOE-18-0520
- Joham, A.E., Teede, H.J., Ranasinha, S., Zoungas, S., Boyle, J., 2015. Prevalence of infertility and use of fertility treatment in women with polycystic ovary syndrome: data from a large community-based cohort study. J Womens Health (Larchmt) 24, 299–307. https://doi.org/10.1089/jwh.2014.5000
- Kamata, H., Honda, S., Maeda, S., Chang, L., Hirata, H., Karin, M., 2005. Reactive Oxygen Species Promote TNFα-Induced Death and Sustained JNK Activation by Inhibiting MAP Kinase Phosphatases. Cell 120, 649–661. https://doi.org/10.1016/j.cell.2004.12.041
- Karim, B.O., Landolfi, J.A., Christian, A., Ricart-Arbona, R., Qiu, W., McAlonis, M., Eyabi, P.O., Khan, K.A., Dicello, J.F., Mann, J.F., Huso, D.L., 2003. Estrous cycle and ovarian changes in a rat mammary carcinogenesis model after irradiation, tamoxifen chemoprevention, and aging. Comp. Med. 53, 532–538.
- Keane, K.N., Cruzat, V.F., Carlessi, R., de Bittencourt, P.I.H., Newsholme, P., 2015. Molecular Events Linking Oxidative Stress and Inflammation to Insulin Resistance and β-Cell Dysfunction [WWW Document]. Oxidative Medicine and Cellular Longevity.

https://doi.org/10.1155/2015/181643

- Kelly, C.C., Lyall, H., Petrie, J.R., Gould, G.W., Connell, J.M., Sattar, N., 2001. Low grade chronic inflammation in women with polycystic ovarian syndrome. J. Clin. Endocrinol. Metab. 86, 2453–2455. https://doi.org/10.1210/jcem.86.6.7580
- Knapp, P., Chabowski, A., Błachnio-Zabielska, A., Jarząbek, K., Wołczyński, S., 2012. Altered Peroxisome-Proliferator Activated Receptors Expression in Human Endometrial Cancer. PPAR Research 2012, 1–5. https://doi.org/10.1155/2012/471524
- Knopfová, L., šMarda, J., 2010. The use of Cox-2 and PPARγ signaling in anti-cancer therapies. Experimental and Therapeutic Medicine 1, 257–264. https://doi.org/10.3892/etm_00000040
- Konstantinopoulos, P.A., Vandoros, G.P., Sotiropoulou-Bonikou, G., Kominea, A., Papavassiliou, A.G., 2007. NF-kappaB/PPAR gamma and/or AP-1/PPAR gamma "on/off" switches and induction of CBP in colon adenocarcinomas: correlation with COX-2 expression. Int J Colorectal Dis 22, 57–68. https://doi.org/10.1007/s00384-006-0112-y
- Lee, J., Kim, M.-S., 2007. The role of GSK3 in glucose homeostasis and the development of insulin resistance. Diabetes Research and Clinical Practice 77, S49–S57. https://doi.org/10.1016/j.diabres.2007.01.033
- Lee, J.Y., Baw, C.-K., Gupta, S., Agarwal, N.A. and A., 2010. Role of Oxidative Stress in Polycystic Ovary Syndrome [WWW Document]. Current Women`s Health Reviews. URL http://www.eurekaselect.com/86322/article (accessed 9.23.19).
- Li, J., Wu, Q., Wu, X.-K., Zhou, Z.-M., Fu, P., Chen, X.-H., Yan, Y., Wang, X., Yang, Z.-W., Li, W.-L., Stener-Victorin, E., Legro, R.S., Ng, E.H.-Y., Zhang, H., Mol, B.W.J., Wang, C.C., for PCOSAct Study Group, 2018. Effect of exposure to second-hand smoke from husbands on biochemical hyperandrogenism, metabolic syndrome and conception rates in women with polycystic ovary syndrome undergoing ovulation induction. Hum. Reprod. 33, 617–625. https://doi.org/10.1093/humrep/dey027
- Livak, K.J., Schmittgen, T.D., 2001. Analysis of relative gene expression data using real-time quantitative PCR and the 2(-Delta Delta C(T)) Method. Methods 25, 402–408. https://doi.org/10.1006/meth.2001.1262
- Lopes, I.M.R.S., Baracat, M.C.P., Simões, M. de J., Simões, R.S., Baracat, E.C., Soares Jr, J.M., 2011. Endometrium in women with polycystic ovary syndrome during the window of implantation. Rev Assoc Med Bras (1992) 57, 702–709.
- Lu, J., Wang, Z., Cao, J., Chen, Y., Dong, Y., 2018. A novel and compact review on the role of oxidative stress in female reproduction. Reprod Biol Endocrinol 16. https://doi.org/10.1186/s12958-018-0391-5
- Macut, D., Bjekić-Macut, J., Savić-Radojević, A., 2013. Dyslipidemia and oxidative stress in PCOS. Front Horm Res 40, 51–63. https://doi.org/10.1159/000341683
- Matsuzaki, T., Tungalagsuvd, A., Iwasa, T., Munkhzaya, M., Yano, K., Mayila, Y., Tokui, T., Yanagihara, R., Matsui, S., Kato, T., Kuwahara, A., Irahara, M., 2017. Clinical outcome of various metformin treatments for women with polycystic ovary syndrome. Reprod Med Biol 16, 179–187. https://doi.org/10.1002/rmb2.12026
- Matthews, D.R., Hosker, J.P., Rudenski, A.S., Naylor, B.A., Treacher, D.F., Turner, R.C., 1985. Homeostasis model assessment: insulin resistance and beta-cell function from fasting plasma glucose and insulin concentrations in man. Diabetologia 28, 412–419. https://doi.org/10.1007/bf00280883
- Meade, E.A., McIntyre, T.M., Zimmerman, G.A., Prescott, S.M., 1999. Peroxisome Proliferators Enhance Cyclooxygenase-2 Expression in Epithelial Cells. Journal of Biological Chemistry 274, 8328–8334. https://doi.org/10.1074/jbc.274.12.8328
- Messinis, I.E., 2005. Ovulation induction: a mini review. Hum. Reprod. 20, 2688–2697. https://doi.org/10.1093/humrep/dei128
- Minge, C.E., Ryan, N.K., Hoek, K.H.V.D., Robker, R.L., Norman, R.J., 2006. Troglitazone Regulates Peroxisome Proliferator-Activated Receptors and Inducible Nitric Oxide Synthase in Murine Ovarian Macrophages. Biol Reprod 74, 153–160.

https://doi.org/10.1095/biolreprod.105.043729

- Motta, A.B., 2010. Dehydroepiandrosterone to induce murine models for the study of polycystic ovary syndrome. J. Steroid Biochem. Mol. Biol. 119, 105–111. https://doi.org/10.1016/j.jsbmb.2010.02.015
- Motta, A.B., Estevez, A., Franchi, A., Perez-Martinez, S., Farina, M., Ribeiro, M.L., Lasserre, A., Gimeno, M.F., 2001. Regulation of lipid peroxidation by nitric oxide and PGF2alpha during luteal regression in rats. Reproduction 121, 631–637. https://doi.org/10.1530/rep.0.1210631
- Murri, M., Luque-Ramírez, M., Insenser, M., Ojeda-Ojeda, M., Escobar-Morreale, H.F., 2013. Circulating markers of oxidative stress and polycystic ovary syndrome (PCOS): a systematic review and meta-analysis. Hum. Reprod. Update 19, 268–288. https://doi.org/10.1093/humupd/dms059
- Nickkho-Amiry, M., McVey, R., Holland, C., 2012. Peroxisome proliferator-activated receptors modulate proliferation and angiogenesis in human endometrial carcinoma. Mol. Cancer Res. 10, 441–453. https://doi.org/10.1158/1541-7786.MCR-11-0233
- Padmanabhan, V., Veiga-Lopez, A., 2013. Sheep models of polycystic ovary syndrome phenotype. Mol. Cell. Endocrinol. 373, 8–20. https://doi.org/10.1016/j.mce.2012.10.005
- Palomba, S., Falbo, A., Chiossi, G., Orio, F., Tolino, A., Colao, A., La Sala, G.B., Zullo, F., 2014. Low-grade chronic inflammation in pregnant women with polycystic ovary syndrome: a prospective controlled clinical study. J. Clin. Endocrinol. Metab. 99, 2942–2951. https://doi.org/10.1210/jc.2014-1214
- Papaioannou, S., Tzafettas, J., 2010. Anovulation with or without PCO, hyperandrogenaemia and hyperinsulinaemia as promoters of endometrial and breast cancer. Best Practice & Research Clinical Obstetrics & Gynaecology, Reproduction and Cancer 24, 19–27. https://doi.org/10.1016/j.bpobgyn.2008.11.010
- Repaci, A., Gambineri, A., Pasquali, R., 2011. The role of low-grade inflammation in the polycystic ovary syndrome. Molecular and Cellular Endocrinology, Endo-Immunology: Interactions between the Immune and Endocrine Systems 335, 30–41. https://doi.org/10.1016/j.mce.2010.08.002
- Sasaki, H., Tanahashi, M., Yukiue, H., Moiriyama, S., Kobayashi, Y., Nakashima, Y., Kaji, M., Kiriyama, M., Fukai, I., Yamakawa, Y., Fujii, Y., 2002. Decreased perioxisome proliferator-activated receptor gamma gene expression was correlated with poor prognosis in patients with lung cancer. Lung Cancer 36, 71–76.
- Schaiff, W.T., Barak, Y., Sadovsky, Y., 2006. The pleiotropic function of PPARγ in the placenta. Molecular and Cellular Endocrinology 249, 10–15. https://doi.org/10.1016/j.mce.2006.02.009
- Sheldrick, E.L.R., Derecka, K., Marshall, E., Chin, E.C., Hodges, L., Wathes, D.C., Abayasekara, D.R.E., Flint, A.P.F., 2007. Peroxisome-proliferator-activated receptors and the control of levels of prostaglandin-endoperoxide synthase 2 by arachidonic acid in the bovine uterus. Biochemical Journal 406, 175–183. https://doi.org/10.1042/BJ20070089
- Sirmans, S.M., Weidman-Evans, E., Everton, V., Thompson, D., 2012. Polycystic ovary syndrome and chronic inflammation: pharmacotherapeutic implications. Ann Pharmacother 46, 403–418. https://doi.org/10.1345/aph.1Q514
- Sobolewski, C., Cerella, C., Dicato, M., Ghibelli, L., Diederich, M., 2010. The Role of Cyclooxygenase-2 in Cell Proliferation and Cell Death in Human Malignancies. International Journal of Cell Biology 2010, 1–21. https://doi.org/10.1155/2010/215158
- Taylor, S.C., Berkelman, T., Yadav, G., Hammond, M., 2013. A defined methodology for reliable quantification of Western blot data. Mol. Biotechnol. 55, 217–226. https://doi.org/10.1007/s12033-013-9672-6
- Taylor, S.C., Posch, A., 2014. The Design of a Quantitative Western Blot Experiment. Biomed Res Int 2014. https://doi.org/10.1155/2014/361590
- van Houten, E.L.A.F., Visser, J.A., 2014. Mouse models to study polycystic ovary syndrome: a possible link between metabolism and ovarian function? Reprod Biol 14,

32–43. https://doi.org/10.1016/j.repbio.2013.09.007

- Wolf, C.J., Hotchkiss, A., Ostby, J.S., LeBlanc, G.A., Gray, L.E., 2002. Effects of prenatal testosterone propionate on the sexual development of male and female rats: a dose-response study. Toxicol. Sci. 65, 71–86. https://doi.org/10.1093/toxsci/65.1.71
- Yang, Y., Qiao, J., Li, R., Li, M.-Z., 2011. Is interleukin-18 associated with polycystic ovary syndrome? Reproductive Biology and Endocrinology 9, 7. https://doi.org/10.1186/1477-7827-9-7
- Yilmaz, M., Bukan, N., Ayvaz, G., Karakoç, A., Törüner, F., Çakir, N., Arslan, M., 2005. The effects of rosiglitazone and metformin on oxidative stress and homocysteine levels in lean patients with polycystic ovary syndrome. Hum Reprod 20, 3333–3340. https://doi.org/10.1093/humrep/dei258
- Zaree, M., Shahnazi, V., Fayezi, S., Darabi, Maryam, Mehrzad-Sadaghiani, M., Darabi, Masoud, Khani, S., Nouri, M., 2015. Expression Levels of PPARγ and CYP-19 in Polycystic Ovarian Syndrome Primary Granulosa Cells: Influence of ω-3 Fatty Acid. Int J Fertil Steril 9, 197–204.
- Zhang, Y., Hu, M., Meng, F., Sun, X., Xu, H., Zhang, J., Cui, P., Morina, N., Li, X., Li, W., Wu, X.-K., Brännström, M., Shao, R., Billig, H., 2017. Metformin Ameliorates Uterine Defects in a Rat Model of Polycystic Ovary Syndrome. EBioMedicine 18, 157–170. https://doi.org/10.1016/j.ebiom.2017.03.023
- Zhao, Y., Zhang, C., Huang, Y., Yu, Y., Li, R., Li, M., Liu, N., Liu, P., Qiao, J., 2015. Up-regulated expression of WNT5a increases inflammation and oxidative stress via PI3K/AKT/NF-κB signaling in the granulosa cells of PCOS patients. J. Clin. Endocrinol. Metab. 100, 201–211. https://doi.org/10.1210/jc.2014-2419
- Zuo, T., Zhu, M., Xu, W., 2016. Roles of Oxidative Stress in Polycystic Ovary Syndrome and Cancers [WWW Document]. Oxidative Medicine and Cellular Longevity. https://doi.org/10.1155/2016/8589318

Highlights:

- Prenatal hyperandrogenization leads to a fetal programming effect in the rat uterus.
- PPAR system and its regulators were altered in the uterine tissue of adult rats.
- A pro-inflammatory environment was created in the uterine tissue of adult rats.
- A misbalanced oxidant/antioxidant state was established in the uterine tissue.